Geoderma 307 (2017) 220–230

Contents lists available at ScienceDirect

Geoderma

journal homepage: www.elsevier.com/locate/geoderma

Sampling designs for soil organic carbon stock assessment of soil profiles

Yakun Zhang, Alfred E. Hartemink*

University of Wisconsin-Madison, Department of Soil Science, FD Hole Soils Lab, 1525 Observatory Drive, Madison, WI 53706, USA

ARTICLE INFO

Keywords:
Fixed depth
Soil horizon
Vertical transect sampling
Fuzzy c-means sampling
vis-NIR spectra
Soil color
Digital soil morphometrics

ABSTRACT

We investigated four sampling designs for soil organic carbon (SOC) stock assessment of soil profiles: (i) sampling by horizons, (ii) vertical transect sampling, (iii) depth-based stratified random sampling, (iv) fuzzy c-means sampling in which we explored the use of vis-NIR spectroscopy, image analysis and color models. An Alfisol and Mollisol profile wall (1 × 1 m) was divided into a 10 × 10 cm raster and 100 samples (about 200 g each) were collected at the centers of grid cells for SOC analysis. Bulk density samples were collected from each 10-cm depth interval along a single vertical transect and the SOC stock was calculated using 100 points in the profile wall. Horizon-based sampling for the Mollisol (5 horizons) ranged from 231 to 262 Mg C ha^{-1}, whereas it ranged from 69 to 99 Mg C ha^{-1} in the Alfisol (3 horizons). The SOC stocks obtained by 1 to 7 vertical transects ranged from 68 to 81 Mg C ha^{-1} in the Alfisol, and 239 to 246 Mg C ha^{-1} in the Mollisol. Depth-based stratified random sampling resulted in the SOC stocks ranging from 77 to 82 Mg C ha^{-1} in the Alfisol and 234 to 257 Mg C ha^{-1} in the Mollisol, and the standard errors decreased with increasing sample size from 10 to 70. Fuzzy c-means clustering created clusters similar to the field delineated horizons. A sample size of 7 in both profiles was sufficient to estimate the mean profile SOC stock by fuzzy c-means sampling. The CIE $L^*a^*b^*$ color model resulted in more accurate estimation in the Alfisol, but the vis-NIR spectra resulted in more accurate estimation in the Mollisol. Soil depth improved the performance of vis-NIR spectra. It is concluded that in these soils, at least two or three vertical transects are required to capture the horizontal variation for estimating profile SOC stock. Depth-wise stratified random sampling reduces the number of samples and is suitable when horizontal variation is high. Fuzzy c-means sampling is useful to determine the minimum sample size for profile SOC stock assessment but requires ancillary data and processing before sampling the soil profile.

1. Introduction

There is a growing need for accurate estimation of soil organic carbon (SOC) stocks (Minasny et al., 2013). Mapping SOC at a range of scales requires pedon data and recent examples have shown the use of such data for estimating SOC stocks across a range of scales (Akpa et al., 2016; Batjes, 2016; Bonfatti et al., 2016b; Priori et al., 2016; Schillaci et al., 2017). Numerous studies assessed SOC stock for the top 30 cm depth which is the standard IPCC sampling depth (IPCC, 2006). Few efforts have been made on profile SOC stock assessment down to 1 m (Lorenz and Lal, 2005). Deep soil carbon is important for enhancing SOC sequestration (Olson and Al-Kaisi, 2015) and affects nitrate and pesticide sorption and leaching behaviors (Meersmans et al., 2009).

From a soil profile, samples can be collected by horizons or by fixed depth intervals (Allen et al., 2010). Marinho et al. (2017) sampled a single vertical transect in a soil pit at 2-cm intervals and derived a depth function. Wang et al. (2017) compared 20-cm fixed-depth sampling and horizon-based sampling. They found that horizon-based sampling resulted in 16–22% higher SOC stocks in the surface (0–20 cm) and 30–40% higher of the whole profile (0–80 cm). Grüneberg et al. (2010) found that sampling by depth interval is preferred for regional SOC stock estimation, whereas sampling by horizon is essential for pedogenesis studies. Boone et al. (1999) demonstrated that sampling by fixed depth intervals is easier to budget and implement, and it is more practical. Vertical sampling design tends to ignore the horizontal variation of soil (Hole, 1953). In order to investigate soil profile variation and produce soil profile maps, raster sampling has been conducted by Davis et al. (1995) with 20 × 20 cm resolution as well as fine grid sampling on soil monoliths (Roudier et al., 2016).

Proximal soil sensing and other instruments have been used to improve soil profile characterization and quantification (Hartemink and Minasny, 2014). In particular, visible near-infrared spectroscopy has shown strong relationships with many soil properties, especially SOC (Stenberg et al., 2010). Lab-based high-resolution vis-NIR imaging spectroscopy has been used for profile C mapping and evaluation of soil profile variation (Schreiner et al., 2015; Steffens and Buddenbaum,

* Corresponding author.
E-mail address: hartemink@wisc.edu (A.E. Hartemink).

http://dx.doi.org/10.1016/j.geoderma.2017.08.013
Received 15 June 2017; Received in revised form 7 August 2017; Accepted 8 August 2017
0016-7061/ Published by Elsevier B.V.

2013). Color is a useful proxy for SOC concentration and can be assessed by Munsell color chart, a digital camera, scanner, and vis-NIR spectroscopy and various studies have estimated SOC from a color model (Stiglitz et al., 2017; Viscarra Rossel et al., 2008; Wills et al., 2007).

There is an increasing need for new soil data for a range of studies, in particular SOC assessment, and there are a range of technologies and approaches being tested in addition to long standing approaches such as in the IPCC. Bonfatti et al. (2016a) used data from 10 pedons to compare four methods for SOC stock estimation: horizon values with discrete data, exponential function, equal-area exponential function, and equal-area quadratic spline function. It was found that different methods produced significantly different results of SOC stocks and values derived from equal-area exponential and equal-area splines were more similar to those of the horizons.

In this paper, we present several sampling approaches for assessing SOC stocks in soil profiles. We have explored different sampling strategies based on sampling soils across the landscape and soil sampling theory and practices. Transect sampling has been used to collect samples along toposequences (Odgers et al., 2008). Stratified random sampling has been used to create strata with similar attributes to improve the sampling efficiency (Webster and Lark, 2012). Stratified sampling like the fuzzy clustering method (de Gruijter et al., 2010), has been used for soil sampling to collect representative calibration dataset for vis-NIR spectra models and digital soil mapping (Ramirez-Lopez et al., 2014; Schmidt et al., 2014). A fuzzy clustering algorithm has been used to delineate soil horizons with vis-NIR spectroscopy by Fajardo et al. (2016). In summary, these approaches have been used to sample two soil profiles and assess the SOC stocks. The objectives of this paper were to: (i) investigate profile sampling designs for profile SOC stock assessment; (ii) evaluate the feasibility of using vis-NIR spectroscopy to estimate SOC in a soil profile; and (iii) explore the possibility of incorporating image analysis and color models for improved sampling and SOC quantification of soil profiles.

2. Materials and methods

2.1. Study area and soil profiles

An Alfisol and Mollisol were studied and sampled in August 2014 and 2015. The Alfisol was located in the Driftless Area of Wisconsin (WGS84 43.03° N, 90.05° W). The altitude of this area is 320 m.a.s.l. The mean annual precipitation is about 860 mm and mean annual temperature is about 7.4 °C. The field was covered by grass at the time of sampling. The soil pit was located at the shoulder position of the landscape with 6% slope. The soil was formed in loess over a mixture of sand, clay, and glauconite weathered from the underlying sandstone, dolomite, and shale bedrock. The soil was classified as fine-silty over clayey, mixed, superactive, mesic Typic Hapludalfs (NewGlarus series). Three horizons were identified in the field down to 1 m depth. Horizon thickness was measured in the middle of the profiles. The Ap horizon (0–22 cm) had granular and subangular blocky structure and silt loam texture, with very dark grayish brown (10YR 3/2, moist) and light brownish gray (10YR 6/2, dry) colors. The Bt horizon (22–68 cm) had subangular blocky structure and silty clay loam texture, with dark yellowish brown (10YR 4/4, moist) and light yellowish brown (10YR 6/4 dry) colors. The 2Bw horizon (68–100 cm) had subangular blocky structure and sandy clay loam texture, with strong brown (7.5YR 4.5/7, moist) and strong brown (7.5YR 5/7 dry) colors.

The Mollisol was located at the University of Wisconsin-Madison West Madison Agricultural Research Station in south-central Wisconsin (WGS84 43.07° N, 89.54° W). The altitude of this area is 330 m.a.s.l. The mean annual precipitation is about 840 mm and mean annual temperature is about 7.8 °C. The field was covered by alfalfa and grass. The soil pit was located at the footslope position and the soil was moderately well-drained to well-drained. The soil was formed in loess over outwash underlain by dolostone bedrock. It was classified as fine-loamy, mixed, superactive, mesic Pachic Argiudolls (Troxel series). Five horizons were identified in the field down to 1 m depth, and the soil contained a buried A horizon at 59 cm depth. The Ap1 horizon (0–18 cm) had granular structure and silt loam texture, with very dark brown (10YR 2/2, moist) and dark grayish brown (10YR 4/2, dry) colors. The Ap2 horizon (18–39 cm) had platy structure and silt loam texture, with very dark brown (10YR 2/2, moist) and dark grayish brown (10YR 4/2, dry) colors. The A2 horizon (39–59 cm) had subangular blocky structure and silt loam texture, with very dark brown (10YR 2/2, moist) and dark grayish brown (10YR 4/2, dry) colors. The thick A-horizon was formed in sediments of eroded topsoils higher in the landscape. The Ab horizon (59–77 cm) had subangular blocky structure and silt loam texture, with black (10YR 2/1, moist) and dark grayish brown (10YR 4/2, dry) colors. The Bt horizon (77–100 cm) had angular blocky structure and silty clay loam texture, with dark yellowish brown (10YR 3/4, moist) and yellowish brown (10YR 5/4, dry) colors (Grauer-Gray and Hartemink, 2016).

2.2. Sample collection and analysis

Soil pits (2 m L × 2 m W × 1.2 m D) were dug and the Alfisol and Mollisol profile walls (1 × 1 m) were divided into a 10 × 10 cm raster. One sample (about 200 g, covering 75% of the raster cell) was collected at the center of each cell for a total of 100 samples. The samples were air-dried, ground, sieved to a diameter smaller than 2 mm. The SOC concentration was determined by dry combustion method with a Flash EA 1112 Series NC Soil Analyzer (Thermo Fisher Scientific Inc.). Bulk density samples were collected at each 10-cm depth interval along a single vertical transect on the left of the soil profile wall assuming that bulk density was uniform across the soil profile. Bulk density was determined by 250 mL rings, and oven-dried bulk soil at 105 °C for 72 h.

2.3. Profile SOC stock

The SOC stock of the 100 grid points was calculated by multiplying SOC concentration, bulk density and 10-cm depth. There were no coarse fragments in the two soils. The SOC stock of each vertical transect was calculated by adding up the SOC stocks for each of the 10 grids. The profile SOC stock was the average of the 10 vertical transects. The grand average SOC stock was used as a standard to compare with the SOC stocks obtained by the four sampling designs.

2.4. vis-NIR spectra collection and analysis

Air dried soil samples were scanned by a portable PSR-3500 vis-NIR spectroradiometer (Spectral Evolution Inc.). The PSR-3500 spectrometer operates in the range of 350–2500 nm with three detectors: (i) a 512-element silicon PDA covering the visible range and part of the near infrared (350–1000 nm) with a resolution of 3 nm; (ii) a 256-element InGaAs array covering 1000–1900 nm with a resolution of 8 nm; and (iii) a 256-element InGaAs array covering 1900–2500 nm with a finer spectral resolution of 6 nm. The reflectance data were resampled to 1 nm for output resulting in 2151 spectral points. The reflectance spectrum was recorded by averaging 50 readings per soil sample measurement, and 3 replicates were taken for each sample by repositioning the probe between each scan. The PSR-3500 was calibrated by a polytetrafluoroethylene (PTEE) white plate with high diffuse reflectance. The vis-NIR spectroradiometer was calibrated every 10 soil samples.

The following preprocessing techniques were implemented on the vis-NIR spectra:

1) The raw reflectance data (R) were converted to absorbance data (A) by A = log (1/R);
2) A second order Savitzky-Golay filter with a smoothing window of 11

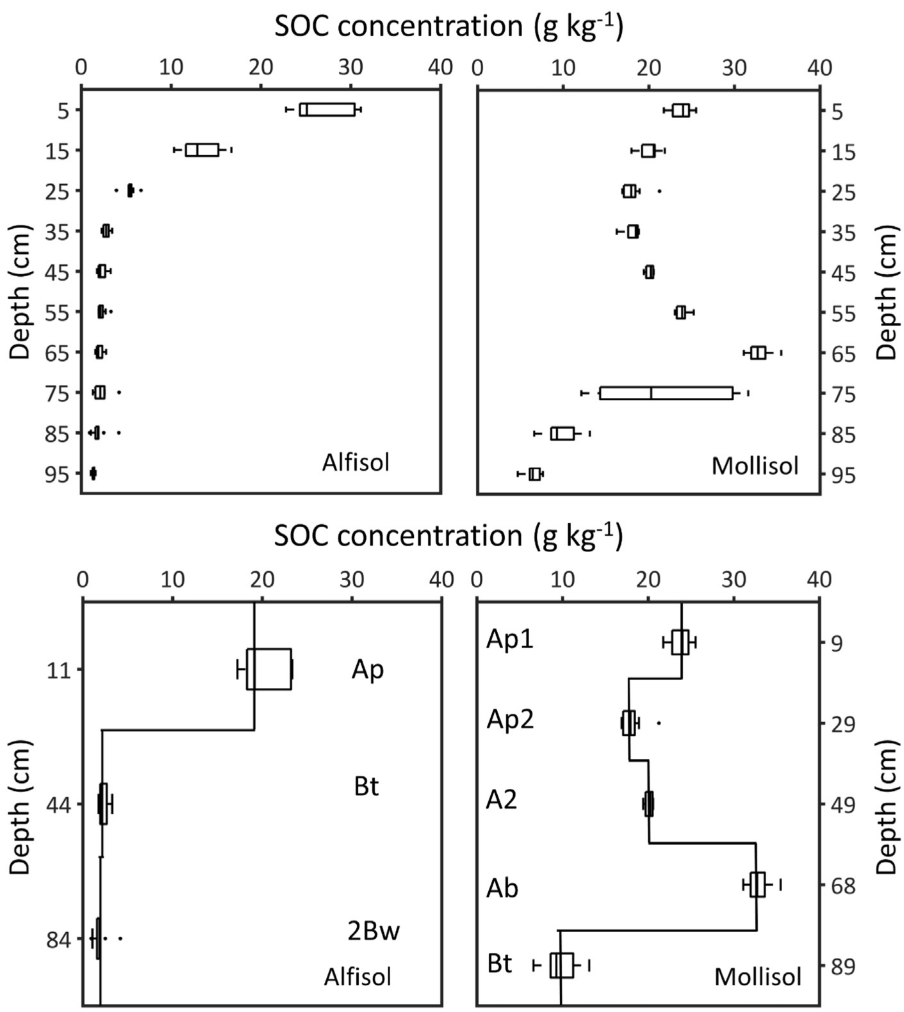

Fig. 1. Distribution of SOC concentration by 10-cm depth intervals (above) and soil horizons (below) of the Alfisol (fine-silty over clayey, mixed, superactive, mesic Typic Hapludalfs, NewGlarus series) and Mollisol (fine-loamy, mixed, superactive, mesic Pachic Argiudolls, Troxel series) in Dane County, Wisconsin. Soil depth at y-axes of horizon graphs indicates center of the horizon.

(Savitzky and Golay, 1964);

3) Selection of every 10th band within the spectral region between 500 and 2450 nm to reduce the high-dimensionality and collinearity.
4) Standard normal variate transformation (SNV) to reduce the light scattering.

A principal component analysis (PCA) was performed on processed spectra to select the first 5 principal components (PCs) for the Alfisol and 3 PCs for the Mollisol, and these explained > 90% of the variation. The cubist model was used to explore the relationship between SOC concentrations and vis-NIR spectra. The 100 samples from each profile were randomly split into calibration dataset (70%) and validation dataset (30%). Coefficient of determination (R^2), root mean squared error (RMSE), bias, residual prediction deviation (RPD), and ratio of performance to inter-quartile distance (RPIQ) were calculated for the calibration and validation. The spectral preprocessing and cubist model were implemented by "prospectr" (Stevens et al., 2013) and "Cubist" (Kuhn et al., 2014) packages in R version 3.3.1.

2.5. Image analysis

Digital images (RAW format) with a horizontal and vertical resolution of 300 dpi were taken for the Alfisol and Mollisol with a Nikon v1 camera. An internal white balance test was executed before the pictures were taken. The digital images were cropped and georeferenced to the profile walls, and processed and scaled to 10 cm resolution in ImageJ (Rasband, 1997). The CIE $L^*a^*b^*$ color model, representing lightness to darkness (L^*), red to green (a^*), and yellow to blue (b^*), were extracted from each pixel of the processed image. The correlations between SOC concentrations and CIE $L^*a^*b^*$ color models were calculated in R version 3.3.1. Multiple linear regression was used to explore the relationship between SOC concentrations and CIE $L^*a^*b^*$ color models and soil depth.

2.6. Sampling designs

Four sampling designs were investigated and the sample support is the 10 × 10 cm grid cell:

1) Sampling by horizons.
   Bulk soil samples are collected at the center of each horizon. In this study, soil horizons were described in the field in the middle of the profiles. The horizon thickness was assumed to be the same across the profile. Then, the soil profile wall was divided into 10 vertical transects (10 cm width). The soil properties of each horizon were represented by the soil properties over 10-cm depth interval at which the horizon centers were located. If the horizon centers were located at the boundary of two 10-cm depths, the soil properties were calculated by averaging the properties from two 10-cm depths. The SOC stock of each vertical transect was calculated by adding up the horizon SOC stocks. The profile SOC stock was expressed by the average SOC stock of 10 vertical transects. The SOC stock of each vertical transect obtained by sampling by horizons was compared with that obtained by sampling by transect (10-cm depth interval).
2) Vertical transect sampling.
   The profile SOC stock was estimated by uniformly distributed

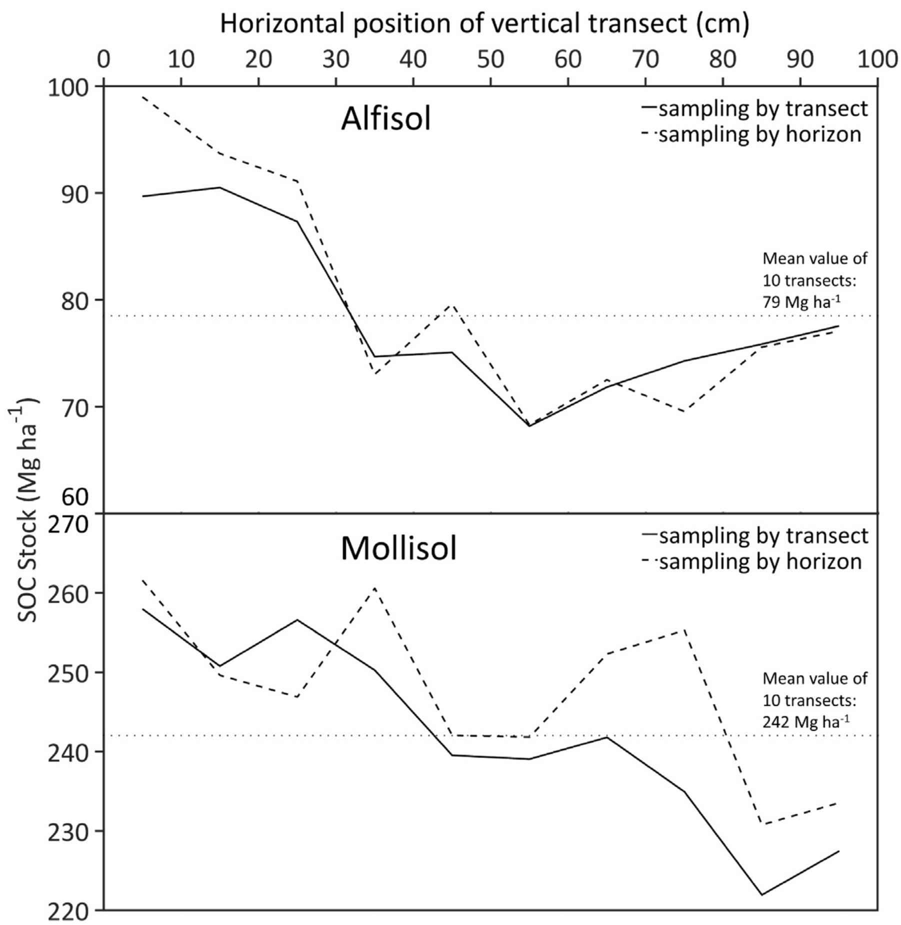

Fig. 2. Alfisol and Mollisol SOC stocks at each horizontal position by sampling by transect (solid line) and by horizons (dashed line).

Table 1
Calibration and validation results of cubist vis-NIR spectral models of SOC concentration (g kg^{-1}) of the Alfisol and Mollisol.

		R^2	RMSE	bias	RPD	RPIQ
Alfisol	Calibration	0.99	0.60	− 0.02	13.55	1.12
	Validation	0.94	1.83	− 0.10	3.97	0.21
Mollisol	Calibration	0.98	1.09	0.02	6.77	2.42
	Validation	0.95	1.70	− 0.05	4.52	2.94

vertical transects with size of 1 to 7, and 10 samples were collected from each 10-cm depth interval in each transect. The profile SOC stock was calculated by the average SOC stock of selected transects.

3) Depth-based stratified random sampling.
The soil profile was divided into 10 layers with 10-cm depth intervals. Samples were randomly taken from each layer with size of 1 to 7. The SOC concentration and bulk density were averaged for each layer and used to calculate SOC stock. The profile SOC stock was calculated by adding up the SOC stocks of 10 layers. The uncertainty (standard error) was obtained by repeating the procedure 50 times.
4) Fuzzy c-means sampling.
Four sets of variables were used for cluster analysis, including (i) 3 or 5 PCs of vis-NIR spectra, (ii) 3 or 5 PCs of vis-NIR spectra and depth, (iii) CIE *L*a*b** color models, and (iv) CIE *L*a*b** color models and depth. The sample with highest membership in each cluster was selected. The sample size was determined by the number of clusters (Schmidt et al., 2014). Cluster sizes varying from 3 to 10 were tested for fuzzy c-means sampling. The SOC stocks of selected sample locations were regarded as representative of clusters and the SOC stock of each cluster was regarded as uniform. Based on the area of clusters and corresponding SOC stocks, the profile SOC stock was calculated. The fuzzy c-means clustering was implemented by "e1071" package (Meyer et al., 2015) in R version 3.3.1. The membership exponent was chosen to be 2.

3. Results

3.1. Profile SOC stocks

In the Alfisol, the SOC concentration decreased exponentially with depth (Fig. 1). The topsoil SOC concentration ranged from 10 to 32 g C kg^{-1} and variation in the subsoil was 1 to 7 g C kg^{-1}. In the Mollisol, the SOC concentration decreased from 25 to 17 g C kg^{-1} down to 30 cm, and increased from 30 to 70 cm. A peak was found at 60 to 70 cm with SOC concentration of 36 g C kg^{-1} in the buried A horizon. SOC concentration decreased to 5 g C kg^{-1} below 70 cm. A large variation (12 to 31 g C kg^{-1}) was observed at 70 to 80 cm soil depth.

In the Alfisol, the SOC stocks decreased from about 90 to 70 Mg C ha^{-1} from left to the middle of the profile and then slightly increased from the middle to the right side (Fig. 2). The profile SOC stock, expressed as the mean of 10 vertical transects, was 79 Mg C ha^{-1} in the Alfisol. In the Mollisol, the SOC stocks of 10 vertical transects decreased from about 260 to 220 Mg C ha^{-1} from left to right in the profile with fluctuations in between. The mean profile SOC stock of the Mollisol was 242 Mg C ha^{-1}.

3.2. Relationship between SOC and vis-NIR spectra, CIE *L*a*b**, and soil depth

The relationship between SOC and vis-NIR spectra, CIE *L*a*b** color model, and soil depth were investigated. The SOC concentration was strongly correlated with vis-NIR spectra in both soils (Table 1). The

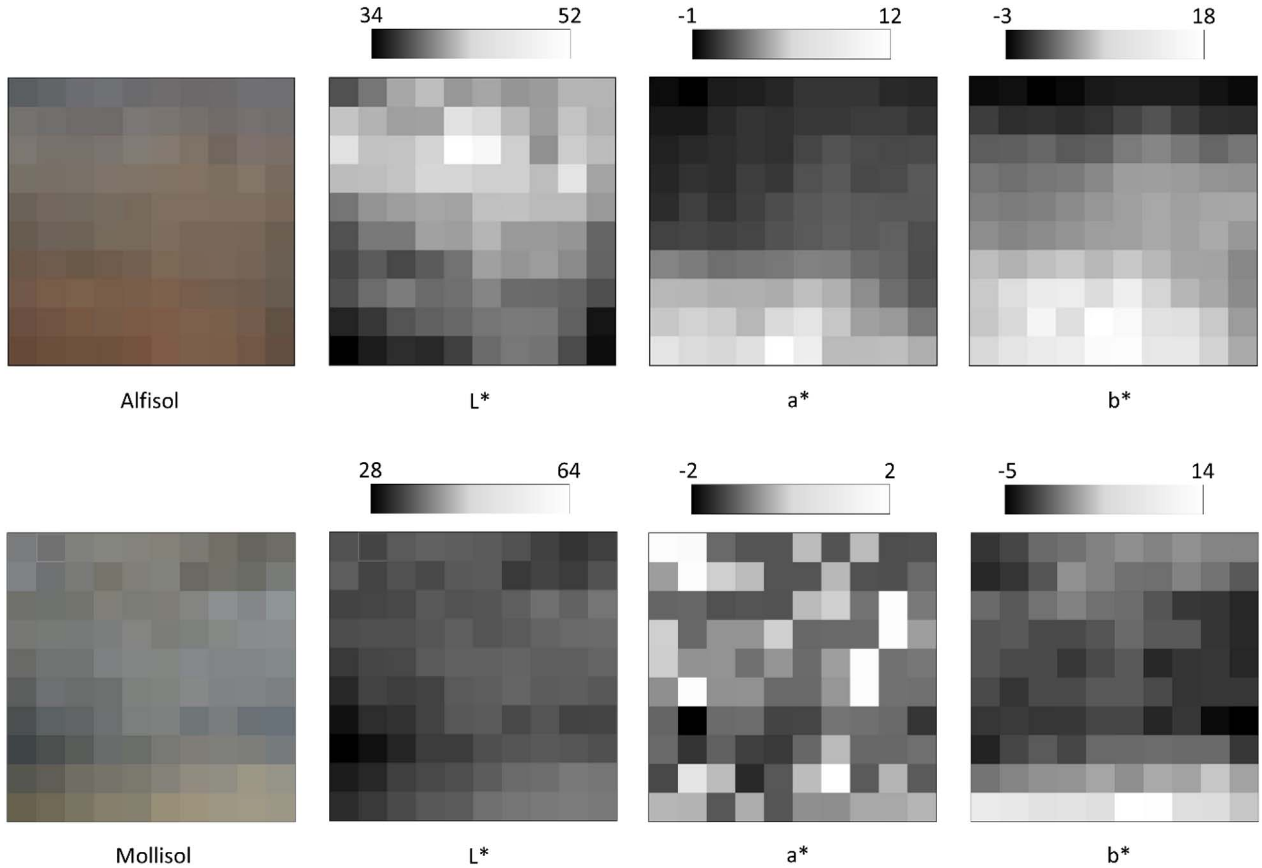

Fig. 3. Alfisol and Mollisol soil profiles and the CIE $L^*a^*b^*$ color coordinates for each 10 × 10 cm pixel.

calibration resulted in slightly better prediction performance with higher R^2 and lower RMSE than validation in both profiles. The Alfisol had higher RPD value in the calibration but lower RPIQ values compared to the Mollisol.

The profile images and CIE $L^*a^*b^*$ color models (10 × 10 cm raster) are shown in Fig. 3. In the Alfisol, the soil color changed from black, to yellowish, and to brownish with depth, corresponding to the Ap, Bt, and 2Bw horizons. The L^* coordinate showed higher values at 0–50 cm depth, and lower values at 50–100 cm depth. The a^* coordinate showed a gradually increasing pattern with depth. The b^* coordinate showed a similar pattern to a^* coordinate, and matched the field delineated horizons. In the Mollisol, a darker layer at 70–80 cm and a yellowish layer at 80–100 cm were observed. The L^* coordinate had lower values at 70–80 cm and in the top right corner which corresponded to the darker color of the image. The a^* coordinate displayed no pattern. The highest b^* coordinate values were in the Bt horizon.

The SOC concentration was negatively correlated to the b^* coordinates (− 0.82 and − 0.74) and a^* coordinates (− 0.55 and − 0.41) in both soils. The L^* coordinate showed a weak positive correlation (0.24) in the Alfisol, but a negative correlation (− 0.43) in the Mollisol. The SOC concentration showed a strong negative correlation (− 0.73) with soil depth in the Alfisol and a weak negative correlation (− 0.39) with soil depth in the Mollisol. Multiple linear regressions of SOC concentration showed significant effects of depths and colors on SOC concentration. Soil depth slightly improved the predictions of SOC concentration compared to colors alone.

Alfisol

$\mathrm{SOC} = 23.99 - 0.16 \times \mathrm{L} + 1.79 \times \mathrm{a}^{***} - 2.11 \times \mathrm{b}^{***}$ $\quad R^2 = 0.82$

$\mathrm{SOC} = 46.77 - 0.20 \times \mathrm{Depth}^{***} - 0.60 \times \mathrm{L}^{***} + 1.89 \times \mathrm{a}^{***} - 1.38 \times \mathrm{b}^{***}$ $\quad R^2 = 0.85$

Mollisol

$\mathrm{SOC} = 31.44 - 0.26 \times \mathrm{L}^{***} - 3.87 \times \mathrm{a}^{**} - 1.23 \times \mathrm{b}^{***}$ $\quad R^2 = 0.67$

$\mathrm{SOC} = 33.90 - 0.05 \times \mathrm{Depth}^{**} - 0.28 \times \mathrm{L}^{***} - 4.24 \times \mathrm{a}^{***} - 1.09 \times \mathrm{b}^{***}$ $\quad R^2 = 0.69$

$^{***} = p < 0.001$, $^{**} = p < 0.01$, $^{*} = p < 0.05$.

3.3. *Sampling designs*

3.3.1. *Sampling by horizons*

The SOC concentrations of each soil horizon are displayed in Fig.1. Sampling by horizons smoothed the within-horizon variations, especially in the Ap horizon of the Alfisol and at 70 to 80 cm depth of the Mollisol. In the Alfisol sampling by horizons showed lower SOC concentration in the Ap horizon. In the Alfisol, the SOC stocks showed similar trends from left to right in the profile compared to the sampling by transect, but SOC stocks were higher in the left 3 vertical transect positions (Fig. 2). The mean profile SOC stock of sampling by horizon was 80 Mg C ha^{-1} of the range 69–99 Mg C ha^{-1}. In the Mollisol, the SOC stocks fluctuated from left to right, and generally had higher values than the stocks obtained by sampling by transect. The SOC stocks obtained by sampling by horizons deviated from the sampling by transect at the right side of the Mollisol profile by 6–20 Mg C ha^{-1}. The mean profile SOC stock of sampling by horizons was 247 Mg C ha^{-1}.

3.3.2. *Vertical transect sampling*

Two sampling schemes of uniformly distributed vertical transects (1 to 7) and corresponding SOC stocks are displayed in Fig. 4. In the Alfisol, 3 to 7 vertical transects sufficed to estimate the mean profile SOC stock. With two transects, the spatially separate transects (A) produced more accurate estimation of profile SOC stock than the clustered two transects (B). Two single transects were selected at the middle of the profile, and both transects produced deviations from the mean profile SOC stock. In the Mollisol, the SOC stocks estimated by 1 to 7 vertical transects ranged from 239 to 246 Mg C ha^{-1}, which slightly deviated from the mean profile SOC stock.

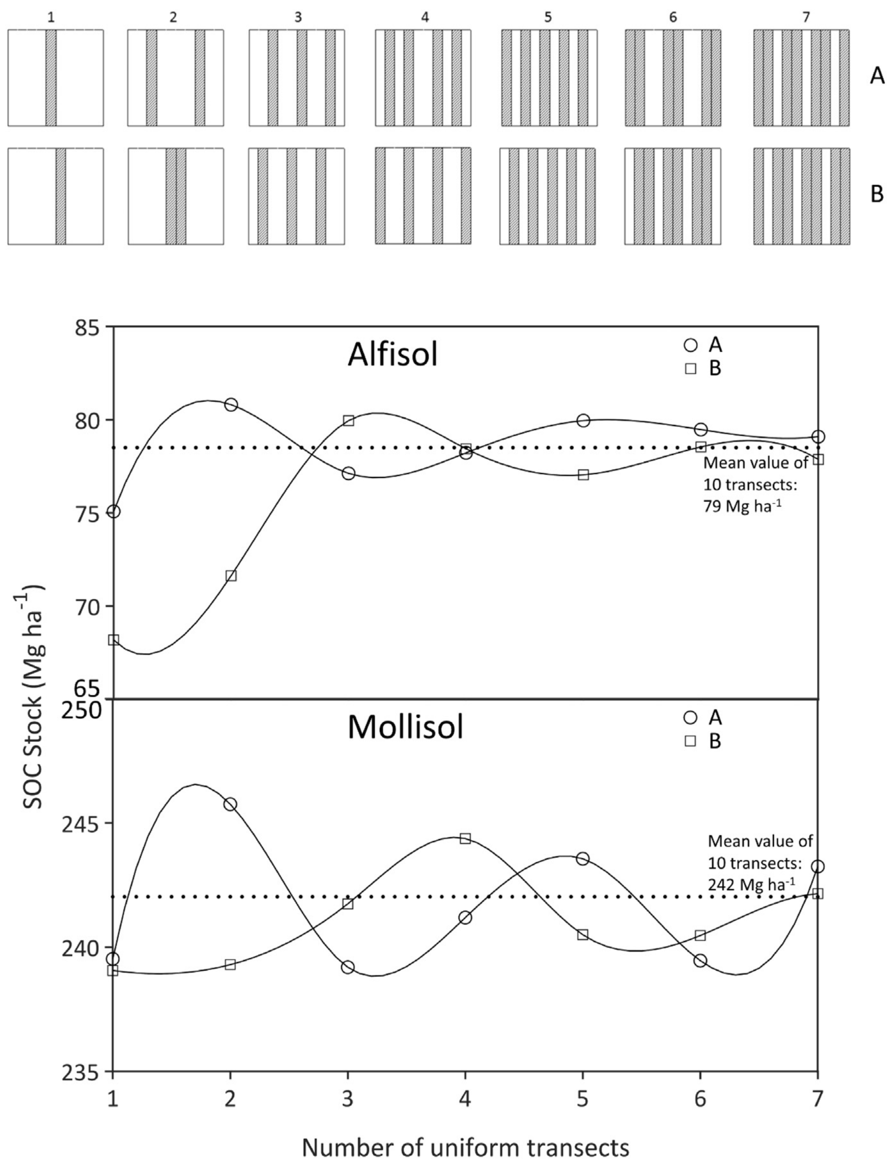

Fig. 4. Uniformly distributed vertical transects and SOC stocks obtained by sampling 1 to 7 transects of the Alfisol and Mollisol. The solid lines were fitted by spline function.

3.3.3. *Depth-based stratified random sampling*

The SOC stocks calculated from depth-based stratified random sampling with 10 to 70 samples are displayed in Fig. 5. In the Alfisol, SOC stocks ranged from 77 to 82 Mg C ha^{-1}, and the standard errors increased from 1 to 5 Mg C ha^{-1} with decreasing sample size from 70 to 10. In the Mollisol, the SOC stocks ranged from 238 to 245 Mg C ha^{-1} using 30 to 70 samples. The SOC stocks were 234 and 257 Mg C ha^{-1} with 20 and 10 samples. The Mollisol showed higher standard errors than the Alfisol, ranging from 2 to 10 Mg C ha^{-1} from 70 to 10 samples.

3.3.4. *Fuzzy c-means sampling*

The hard clusters and sampling points of fuzzy c-means sampling with 3 to 10 samples of the Alfisol and Mollisol are presented in Fig. 6. In both profiles, the spectra displayed more vertical variation, whereas CIE $L^*a^*b^*$ produced more irregularities. Soil depth tended to create more horizontal uniformities compared to spectra or CIE $L^*a^*b^*$ alone. The clusters are similar to the field delineated horizons with a cluster size < 5. In the Alfisol, the 3-cluster scheme showed a similar pattern in 2Bw horizon, but a deeper Ap horizon. The 4-cluster scheme displayed similar patterns in Ap and 2Bw horizons, but split the Bt horizon into two horizons. In the Mollisol, the three clusters generated by spectra and depth matched with Ap1 and Ap2, A2 and Ab, and Bt horizons. The four clusters generated by spectra and depth matched with the Ap1, Ap2, A2 + Ab, and Bt horizons. The five clusters generated by spectra and depth and CIE $L^*a^*b^*$ and depth matched the field delineated horizons of the Mollisol. In both soil profiles, more clusters resulted in finer within-horizon partitions.

The SOC stocks obtained by fuzzy c-means sampling with 3 to 10 samples in the Alfisol and Mollisol are plotted in Fig. 7. With a sample size is < 6, the SOC stocks deviated from the mean but a sample size of 7 in both profiles was sufficient to estimate the mean with < 10% deviation. In the Alfisol, CIE $L^*a^*b^*$ resulted in more accurate mean profile SOC stock estimation than solely the use of spectra. Soil depth improved the performance of spectra, but had no improvements on the performance of CIE $L^*a^*b^*$. In the Mollisol, the spectra resulted in more accurate estimation than CIE $L^*a^*b^*$. The soil depth optimized the estimation with spectra, but resulted in an overestimation with the use of CIE $L^*a^*b^*$.

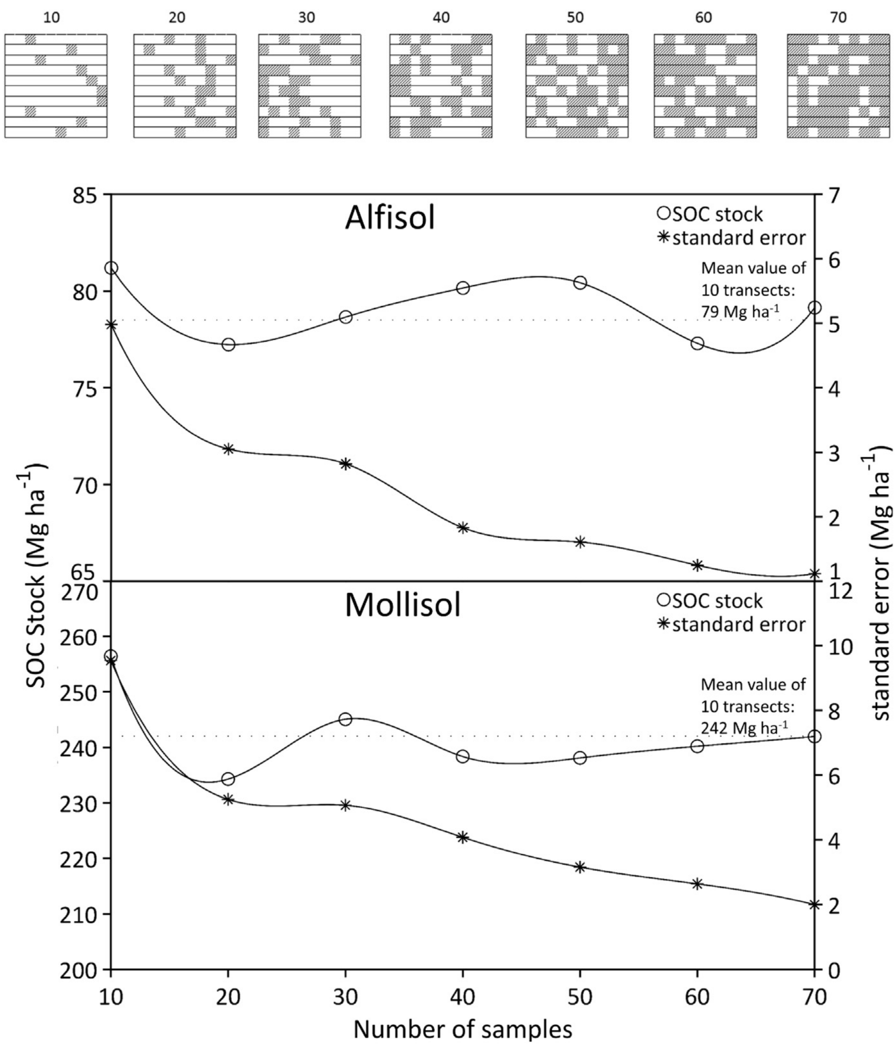

Fig. 5. SOC stocks obtained by depth-based stratified random sampling with 10 to 70 samples and standard errors obtained by 50 times repeated random sampling processes of the Alfisol and Mollisol. Note different scales of SOC stocks and standard error axes. The solid lines were fitted by spline function.

4. Discussion

4.1. Sampling by horizons or by fixed depth

SOC stock estimation was affected by the variation in horizon thickness. In the Alfisol, three horizons were identified at 0–22 cm, 22–68 cm, and 68–100 cm at the middle of the profile. The thickness of Ap horizon increased from left to right in the profile, and consequently the thickness of 2Bw horizon decreased. The Ap horizon is 10 cm thinner on the left side of the soil profile, leading to 10% higher SOC stock by horizon-based sampling. Variation in the depth of the plough layer and bulk density are the most important sources of field-scale SOC stock variability in cropland (Goidts et al., 2009). Premrov et al. (2017) suggested that sampling by horizons with accurate measurements of horizon thickness is a suitable method for SOC stock estimation.

In the Mollisol, 5 horizons were delineated at 0–18 cm, 18–39 cm, 39–59 cm, 59–77 cm, and 77–100 cm. The deviation of SOC stocks obtained by horizon sampling from fixed-depth sampling was due to the selection of representative depths of the corresponding horizons. The data from 0 to 10 cm were used to represent Ap horizon (0–18 cm) which resulted in an overestimation of SOC stocks. Palmer et al. (2002) illustrated that changes in carbon content within A horizon affect SOC stock estimation. They found that the SOC concentrations were 1.5% for 0–5 cm and 0.8% for 5–10 cm, but the SOC concentration of bulk soil over A horizon (0–12 cm) was 1.2%. Within-horizon variation was ubiquitous and we suggest that samples are collected at the center of the horizon or bulk samples of the entire horizon.

4.2. Vertical transect sampling

Vertical transects were uniformly distributed across the profile to explore the variation in the profile. The accuracy of vertical transect sampling is influenced by the horizontal variation of profiles. In the Alfisol, the SOC stocks decreased from left to middle in the profile, and then increased from middle to right in the profile. Three or more vertical transects captured the variations at the left, middle, and right of the profile, resulting in an accurate estimation of the profile SOC stock. With two vertical transects, the spatially separate transects (A) captured the variation, and led to more accurate estimation than the clustered two transects (B). In the Mollisol, SOC stocks decreased from left to right in the profile. The lower variation pattern compared to the Alfisol resulted in a better estimation in the Mollisol by two vertical transects or a single vertical transect.

The horizontal variation of profiles implied that the sampling with a single core is not sufficient to capture the short range variation (Hole, 1953). Since the actual horizontal variation of soil profile is unknown, our research seems to suggest that 2, 3, or 4 cores or vertical transects may be sampled or composited at lines, equilateral triangular grids, and square grids to capture the variation in these soil profiles.

4.3. Depth-based stratified random sampling

SOC concentration typically decreases exponentially with depth (Jenny, 1930) and such a pattern was observed in the Alfisol. The Mollisol with the buried horizon had a more complex depth function.

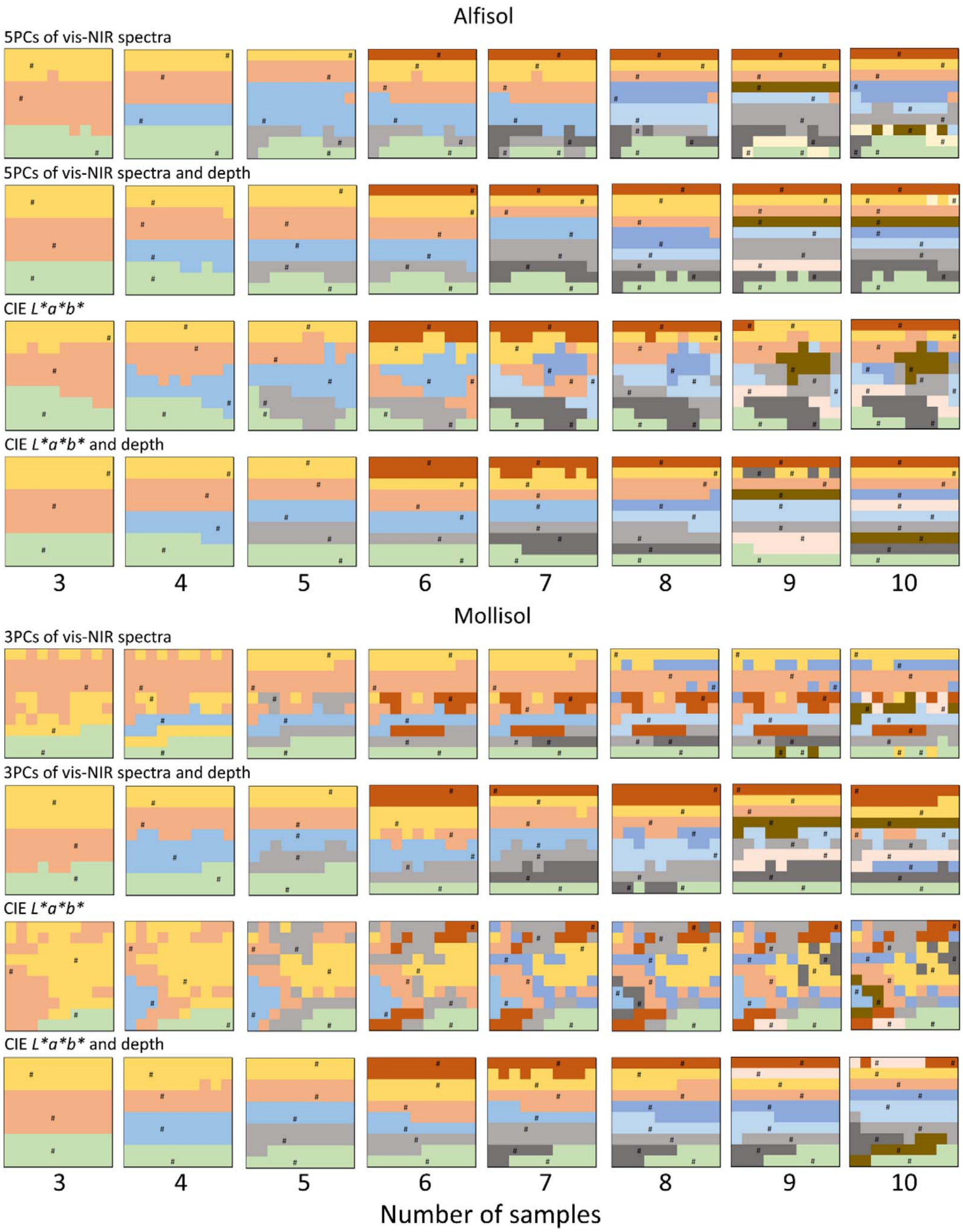

Fig. 6. Hard clusters and sampling points (#) of fuzzy c-means sampling with 3 to 10 samples of the Alfisol and Mollisol. Fuzzy c-means clustering was implemented on 5 or 3 principal components (PCs) of vis-NIR spectra, 5 or 3 PCs of vis-NIR spectra and depth, CIE $L^*a^*b^*$ color models, and CIE $L^*a^*b^*$ color models and depth, respectively. Sampling points were selected from each cluster with highest membership.

The random procedure increased the flexibility of vertical transect sampling and tended to capture more horizontal variation. In the Alfisol, the standard errors were 5 and 3 Mg C ha^{-1} with 10 and 20 samples, and a better estimation of the SOC stock was obtained compared to vertical transect sampling with same size. In the Mollisol, large standard errors and deviations with 10 and 20 samples were observed in the stratified random sampling that did not perform well compared to the vertical transect sampling. This suggests that depth-based stratified random sampling is more flexible and effective when the horizontal variation is high. When the sample size is 30 or more, either sampling design results in a good estimation of the SOC stocks.

4.4. Fuzzy clustering

The vis-NIR spectra were well correlated with SOC concentration. The carbon-spectra relationship is partly due to the colorimetric feature of C in the visible region (Stenberg et al., 2010). The b^* coordinate showed good negative correlation with SOC concentration which was comparable to other studies (Stiglitz et al., 2017; Viscarra Rossel et al., 2008). The b^* coordinate represented the chromatic parameter from blue to yellow and mainly expressed the yellowish color in the subsoil which corresponded to the low SOC concentration. The distribution of the b^* coordinate matched the delineated horizons which contributes to the usefulness of clustering analysis. The a^* coordinate exhibited stronger correlation in the Alfisol than that in the Mollisol which may be due to the brownish color of the 2Bw horizon in the Alfisol. The L^* coordinate showed low correlation with SOC concentration which was comparable to Stiglitz et al. (2017), but it was lower than Viscarra Rossel et al. (2008). Several studies have used depth to improve the prediction of SOC by CIE $L^*a^*b^*$ alone (Stiglitz et al., 2017; Wills et al., 2007) but it seems to marginally improve the SOC prediction by multiple linear regression.

The results showed that the fuzzy c-means sampling can be used to collect representative samples for profile SOC stock assessment. The vis-

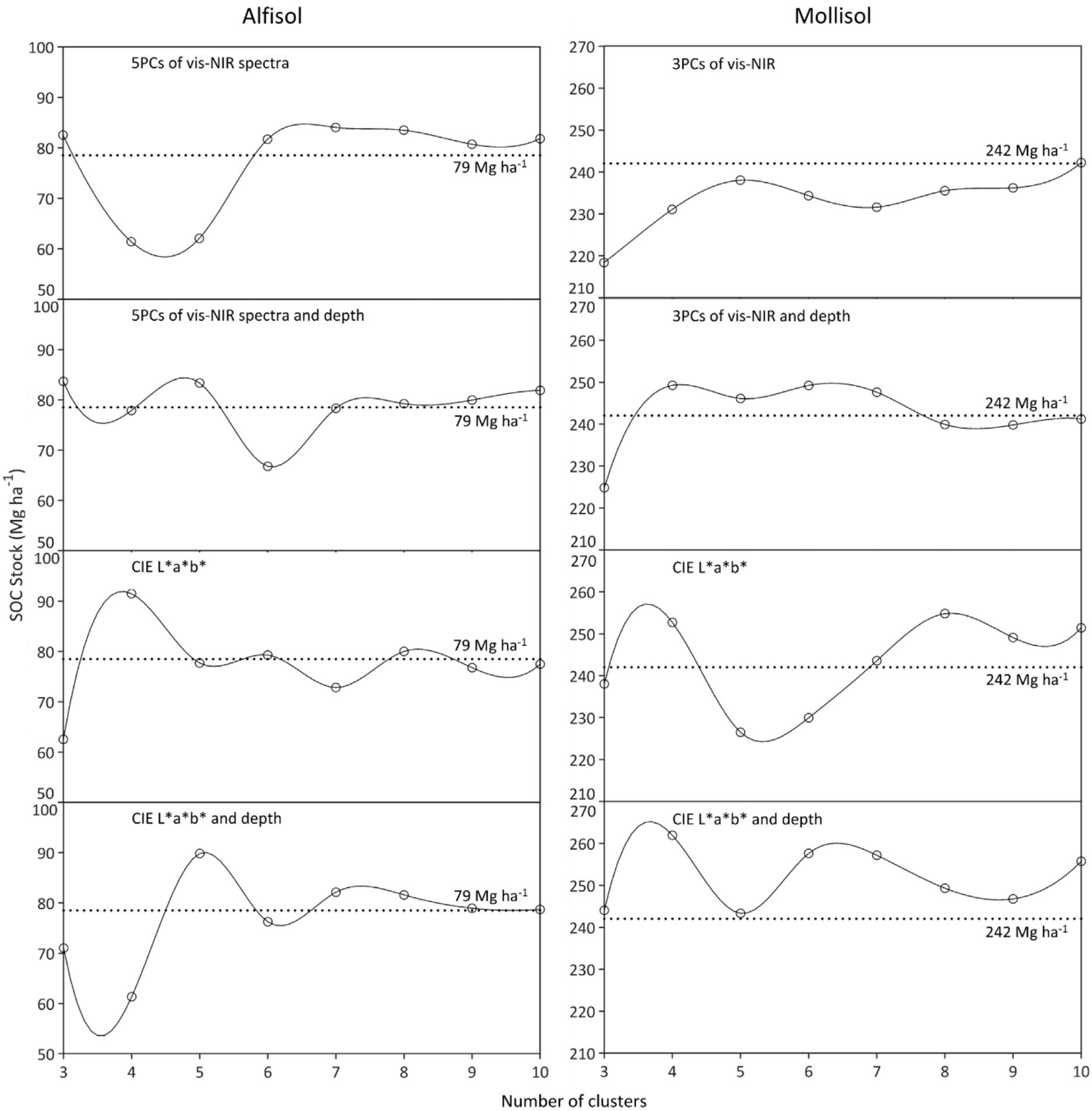

Fig. 7. SOC stocks obtained by fuzzy c-means sampling with 3 to 10 samples of the Alfisol and Mollisol. The solid lines were fitted by spline function.

Table 2
Summary of profile sampling designs for SOC stock assessment used in this study.

Sampling design	Ancillary variables	Minimum sample size	Summary
Sampling by horizons	No	2 or 3 transects and horizon-based samples	Soil horizons are accurately delineated and horizon thickness are measured. Representative samples are collected at the center of the horizon or bulk samples of the entire horizon.
Vertical transect sampling	No	2 or 3 vertical transects at 10-cm fixed intervals	Two or three vertical transects (cores) are required or composited in vertical transect sampling to capture the short range horizontal variations. The depth interval is usually 10 cm when actual soil samples are taken. Smaller increments can be measured *in situ* or on soil cores.
Depth-based stratified random sampling	No	10 or 20 samples	It increases the flexibility and estimation accuracy when the horizontal variation is large and SOC concentration decreases with depth.
Fuzzy c-means sampling	Vis-NIR spectra Color models	3 more samples than delineated horizons	This is a two-step sampling design whereby the ancillary variables are collected and processed in the first step, and samples are collected after the first step. It requires specific equipment and data analysis.

NIR spectra was more effective than the CIE $L^*a^*b^*$ color model with the consideration of clustering. The soil depth helped to improve the vertical partitioning of profiles and the SOC stock estimation. When the sample size is small, clustering analysis generated clusters that matched delineated horizons and resulted in accurate estimation of SOC stock in the Mollisol. When the cluster size is large, the clustering analysis showed no match to the horizonation, but it contributed to the estimation of profile SOC stock.

Roubens (1982) compared clustering validity indices and recommended the fuzziness performance index and normalized classification entropy which have been used by others to determine the optimal cluster size (McBratney and Moore, 1985; Odeh et al., 1992). Such indices may indicate smaller cluster size than it is actually required. McBratney and Moore (1985) applied these two indices on a dataset from China which indicated that two clusters was the "best" solution. They used six clusters to achieve finer partition for practical use. Therefore, in horizon delineation, the minimum cluster size may be determined by number of horizons that are identified in the field and using the indices. But for the purpose of estimating profile SOC stock, a few more samples may be needed (a total of 7 samples in the Alfisol and Mollisol) to achieve 90% estimation accuracy.

5. Conclusions

This study presented four sampling designs for soil profile SOC stock assessment. The following can be concluded (Table 2):

1) Horizon-based sampling is effective to assess profile SOC stock provided (i) horizon depths are accurately measured across the soil profile wall; (ii) representative samples are collected at the horizon centers or bulk samples of the entire horizons.
2) Two or three vertical transects (cores) are required or composited in vertical transect sampling to capture the horizontal variations.
3) Depth-wise stratified random sampling increases the flexibility and the estimation accuracy of vertical transect sampling when the horizontal variation is high. It is suitable when the SOC concentration decreases with depth.
4) Fuzzy c-means sampling can be used to stratify the soil profile and determine representative samples. Both vis-NIR spectra and CIE $L^*a^*b^*$ color model were effective variables for clustering analysis, but color parameters created irregular patches of the profiles. The soil depth improved the profile partitioning and SOC stock estimation by spectra or color models alone. The accuracy increased with increasing cluster size. A small sample size which is determined by the identified horizons may be appropriate for horizonation, whereas more samples are required to improve the accuracy. However, fuzzy c-means sampling requires specific equipment (spectrometer or digital camera). It is a two-step sampling design whereby the ancillary variables are collected and processed in the first step followed by sample collection in the field.

We suggest 2 or 3 vertical transects be sampled or composited in a soil pit. In these soils, uniformly distributed vertical transect sampling or depth-based stratified random sampling are both suitable methods for SOC stock estimation. Fuzzy c-means sampling needs slightly more samples (*e.g.* 3) than delineated horizon to achieve > 90% estimation accuracy.

Acknowledgements

This research was partly supported by a Hatch project of the National Institute of Food and Agriculture, United States Department of Agriculture, accession number 1003083.

References

Akpa, S.I.C., Odeh, I.O.A., Bishop, T.F.A., Hartemink, A.E., Amapu, I.Y., 2016. Total soil organic carbon and carbon sequestration potential in Nigeria. Geoderma 271, 202–215.
Allen, D.E., Pringle, M.J., Page, K.L., Dalal, R.C., 2010. A review of sampling designs for the measurement of soil organic carbon in Australian grazing lands. Rangel. J. 32, 227–246.
Batjes, N.H., 2016. Harmonized soil property values for broad-scale modelling (WISE30sec) with estimates of global soil carbon stocks. Geoderma 269, 61–68.
Bonfatti, B.R., Hartemink, A.E., Giasson, E., 2016a. Comparing soil C stocks from soil profile data using four different methods. In: Hartemink, A.E., Minasny, B. (Eds.), Digital Soil Morphometrics. Springer International Publishing, Dordrecht, pp. 315–329.
Bonfatti, B.R., Hartemink, A.E., Giasson, E., Tornquist, C.G., Adhikari, K., 2016b. Digital mapping of soil carbon in a viticultural region of Southern Brazil. Geoderma 261, 204–221.
Boone, R.D., Grigal, D.F., Sollins, P., Ahrens, R.J., Armstrong, D.E., 1999. Soil Sampling, Preparation, Archiving, and Quality Control. Standard Soil Methods for Long-Term Ecological Research. Oxford University Press, New York.
Davis, J.G., Hossner, L.R., Wilding, L.P., Manu, A., 1995. Variability of soil chemical properties in two sandy, dunal soils of Niger. Soil Sci. 159, 321–330.
de Gruijter, J.J., McBratney, A.B., Taylor, J., 2010. Sampling for High-Resolution Soil Mapping, Proximal Soil Sensing. Springerpp. 3–14.
Fajardo, M., McBratney, A., Whelan, B., 2016. Fuzzy clustering of Vis-NIR spectra for the objective recognition of soil morphological horizons in soil profiles. Geoderma 263, 244–253.
Goidts, E., van Wesemael, B., Crucifix, M., 2009. Magnitude and sources of uncertainties in soil organic carbon (SOC) stock assessments at various scales. Eur. J. Soil Sci. 60, 723–739.
Grauer-Gray, J.R., Hartemink, A.E., 2016. Variation of soil properties in a Mollisol profile wall. In: Hartemink, A.E., Minasny, B. (Eds.), Digital Soil Morphometrics. Springer International Publishing, Dordrecht, pp. 165–189.
Grüneberg, E., Schöning, I., Kalko, E.K.V., Weisser, W.W., 2010. Regional organic carbon stock variability: a comparison between depth increments and soil horizons. Geoderma 155, 426–433.
Hartemink, A.E., Minasny, B., 2014. Towards digital soil morphometrics. Geoderma 230, 305–317.
Hole, F.D., 1953. Suggested terminology for describing soils as three-dimensional bodies. Soil Sci. Soc. Am. J. 17, 131–135.
IPCC, 2006. 2006 IPCC Guidelines for National Greenhouse Gas Inventories. Intergovernmental Panel on Climate Change.
Jenny, H., 1930. Study on the Influence of Climate Upon the Nitrogen and Organic Matter Content of the Soil.
Kuhn, M., Weston, S., Keefer, C., Coulter, N., Quinlan, R., 2014. Cubist: rule-and instance-based regression modeling. In: R Package Version 0.0.18.
Lorenz, K., Lal, R., 2005. The depth distribution of soil organic carbon in relation to land use and management and the potential of carbon sequestration in subsoil horizons. Adv. Agron. 88, 35–66.
Marinho, M.A., Pereira, M.W.M., Vázquez, E.V., Lado, M., González, A.P., 2017. Depth distribution of soil organic carbon in an oxisol under different land uses: stratification indices and multifractal analysis. Geoderma 287, 126–134.
McBratney, A.B., Moore, A.W., 1985. Application of fuzzy sets to climatic classification. Agric. For. Meteorol. 35, 165–185.
Meersmans, J., van Wesemael, B., De Ridder, F., Van Molle, M., 2009. Modelling the three-dimensional spatial distribution of soil organic carbon (SOC) at the regional scale (Flanders, Belgium). Geoderma 152, 43–52.
Meyer, D., Dimitriadou, E., Hornik, K., Weingessel, A., Leisch, F., 2015. e1071: Misc functions of the Department of Statistics (e1071), TU Wien. In: R Package Version 1.6-7, Retrieved from.
Minasny, B., McBratney, A.B., Malone, B.P., Wheeler, I., 2013. Digital mapping of soil carbon. Adv. Agron. 118, 1–47.
Odeh, I.O.A., Chittleborough, D.J., McBratney, A.B., 1992. Soil pattern recognition with fuzzy-c-means: application to classification and soil-landform interrelationships. Soil Sci. Soc. Am. J. 56, 505–516.
Odgers, N.P., McBratney, A.B., Minasny, B., 2008. Generation of kth-order random toposequences. Comput. Geosci. 34, 479–490.
Olson, K.R., Al-Kaisi, M.M., 2015. The importance of soil sampling depth for accurate account of soil organic carbon sequestration, storage, retention and loss. Catena 125, 33–37.
Palmer, C.J., Smith, W.D., Conkling, B.L., 2002. Development of a protocol for monitoring status and trends in forest soil carbon at a national level. Environ. Pollut. 116 (Supplement 1), S209–S219.
Premrov, A., Cummins, T., Byrne, K.A., 2017. Assessing fixed depth carbon stocks in soils with varying horizon depths and thicknesses, sampled by horizon. Catena 150, 291–301.
Priori, S., Fantappie, M., Bianconi, N., Ferrigno, G., Pellegrini, S., Costantini, E.A.C., 2016. Field-scale mapping of soil carbon stock with limited sampling by coupling gamma-ray and vis-NIR spectroscopy. Soil Sci. Soc. Am. J. 80, 954–964.
Ramirez-Lopez, L., Schmidt, K., Behrens, T., van Wesemael, B., Demattê, J.A.M., Scholten, T., 2014. Sampling optimal calibration sets in soil infrared spectroscopy. Geoderma 226–227, 140–150.
Rasband, W., 1997. ImageJ. US National Institutes of Health, Bethesda, MD.
Roubens, M., 1982. Fuzzy clustering algorithms and their cluster validity. Eur. J. Oper. Res. 10, 294–301.
Roudier, P., Manderson, A., Hedley, C., 2016. Advances towards quantitative assessments of soil profile properties. In: Hartemink, A.E., Minasny, B. (Eds.), Digital Soil Morphometrics. Springer International Publishing, Dordrecht, pp. 113–132.
Savitzky, A., Golay, M.J., 1964. Smoothing and differentiation of data by simplified least squares procedures. Anal. Chem. 36, 1627–1639.
Schillaci, C., Lombardo, L., Saia, S., Fantappiè, M., Märker, M., Acutis, M., 2017. Modelling the topsoil carbon stock of agricultural lands with the stochastic gradient treeboost in a semi-arid Mediterranean region. Geoderma 286, 35–45.
Schmidt, K., Behrens, T., Daumann, J., Ramirez-Lopez, L., Werban, U., Dietrich, P., Scholten, T., 2014. A comparison of calibration sampling schemes at the field scale.

Geoderma 232–234, 243–256.
Schreiner, S., Buddenbaum, H., Emmerling, C., Steffens, M., 2015. VNIR/SWIR laboratory imaging spectroscopy for wall-to-wall mapping of elemental concentrations in soil cores. Photogrammetrie, Fernerkundung, Geoinformation 2015, 423–435.
Steffens, M., Buddenbaum, H., 2013. Laboratory imaging spectroscopy of a stagnic luvisol profile — high resolution soil characterisation, classification and mapping of elemental concentrations. Geoderma 195–196, 122–132.
Stenberg, B., Viscarra Rossel, R.A., Mouazen, A.M., Wetterlind, J., 2010. Visible and near infrared spectroscopy in soil science. Adv. Agron. 107, 163–215.
Stevens, A., Ramirez-Lopez, L., Stevens, M.A., Rcpp, L., 2013. Prospectr: miscellaneous functions for processing and sample selection of vis-NIR diffuse reflectance data. In: R Package Version 0.1.3, pp. 32.
Stiglitz, R., Mikhailova, E., Post, C., Schlautman, M., Sharp, J., 2017. Using an inexpensive color sensor for rapid assessment of soil organic carbon. Geoderma 286, 98–103.
Viscarra Rossel, R.A., Fouad, Y., Walter, C., 2008. Using a digital camera to measure soil organic carbon and iron contents. Biosyst. Eng. 100, 149–159.
Wang, H.M., Wang, W.J., Chang, S.X., 2017. Sampling method and tree-age affect soil organic C and N contents in larch plantations. Forest 8, 15.
Webster, R., Lark, M., 2012. Field Sampling for Environmental Science and Management. Routledge.
Wills, S.A., Burras, C.L., Sandor, J.A., 2007. Prediction of soil organic carbon content using field and laboratory measurements of soil color. Soil Sci. Soc. Am. J. 71, 380–388.